J|A|C|S
ARTICLES

Published on Web 11/11/2010

Bridging the Gap between Electrochemical and Organometallic Activation: Benzyl Chloride Reduction at Silver Cathodes

Yi-Fan Huang,[†] De-Yin Wu,[†] An Wang,[†] Bin Ren,[†] Sandra Rondinini,[‡] Zhong-Qun Tian,*[,†] and Christian Amatore*[,§]

State Key Laboratory of Physical Chemistry of Solid Surfaces and College of Chemistry and Chemical Engineering, Xiamen University, 361005 Xiamen, China, Dipartimento di Chimica Fisica ed Elettrochimica, Università degli Studi di Milano, Via Golgi 19, 20133 Milan, Italy, and Département de Chimie, Ecole Normale Supérieure, UMR 8640, 24 Rue Lhomond, F-75231 Paris Cedex 5, France

Received July 20, 2010; E-mail: christian.amatore@ens.fr; zqtian@xmu.edu.cn

Abstract: Integration of voltammetry, surface-enhanced Raman spectroscopy (SERS), and density functional theory (DFT) has allowed unraveling the mechanistic origin of the exceptional electrocatalytic properties of silver cathodes during the reduction of benzyl chloride. At inert electrodes the initial reduction proceeds through a concerted direct electron transfer yielding a benzyl radical as the first intermediate. Conversely, at silver electrodes it involves an uphill preadsorption of benzyl chloride onto the silver cathode. Reduction of this adduct affords a species tentatively described as a distorted benzyl radical anion stabilized by the silver surface. This transient species rapidly evolves to yield ultimately a benzyl radical bound onto the silver surface, the latter being reduced into a benzyl−silver anionic adduct which eventually dissociates into a free benzyl anion at more negative potentials. Within this framework, the exceptional electrocatalytic properties of silver cathodes stem from the fact that they drastically modify the mechanism of the 2e-reduction pathway through a direct consequence of the electrophilicity of silver cathode surfaces toward organic halides. This mechanism contrasts drastically with any of those tentatively invoked previously, and bridges classical electroreduction mechanisms and oxidative additions similar to those occurring during organometallic homogeneous activation of organic halides by low-valent transition-metal complexes.

Introduction

Benzyl chloride ($PhCH_2Cl$) reduction has attracted a large amount of attention in electrochemical investigations of electron-transfer mechanisms because it represents a paradigm in which the carbon−chlorine bond which is reductively cleaved is significantly coupled with an aromatic system.[1] For this reason the unraveling of its exact reduction mechanism at inert electrodes[2a] has played an important role in the delineation between concerted and nonconcerted pathways in electrochemistry.[2] Yet, it has been recently reported that the reduction of organic halides is greatly facilitated by specific metallic cathodes (Ag, Pd, Cu)[3−6] compared to inert electrodes such as glassy carbon.[2a] Silver cathodes present the highest electrocatalytic properties among them. Hence, the reduction of benzyl chloride

[†] Xiamen University.
[‡] Università degli Studi di Milano.
[§] Ecole Normale Supérieure.

(1) In the classical view the nonconcerted reductive cleavage of aromatic halides proceeds by electron injection into the low energy π^* aryl orbital. This is then transferred into the σ^* C−Cl one when its energy becomes reduced following its vibrational elongation. However, this does not account for the requirement of a significant overlap between the two molecular orbitals which remain orthogonal in such a process. Thus, an out-of-plane bending of the C−Cl bond in PhCl was shown recently to be crucial for allowing the cleavage of the C−Cl bond. See the following: (a) Laage, D.; Burghardt, I.; Sommerfeld, T.; Hynes, J. T. *J. Phys. Chem.* **2003**, *107*, 11271–11291. (b) Burghardt, I.; Laage, D.; Hynes, J. T. *J. Phys. Chem.* **2003**, *107*, 11292–11306. In benzyl halides, the π^* and σ^* are nonorthogonal and have a sufficient overlap to allow a direct electron-transfer into the conjugated orbital hence leading to a "concerted" rupture of the carbon−halide bond.

(2) (a) Andrieux, C. P.; Gorande, A. L.; Savéant, J.-M. *J. Am. Chem. Soc.* **1992**, *114*, 6892–6904. (b) Cardinale, A.; Isse, A. A.; Gennaro, A.; Robert, M.; Savéant, J.-M. *J. Am. Chem. Soc.* **2002**, *124*, 13533–13539. (c) Isse, A. A.; Gennaro, A. *J. Phys. Chem. A* **2004**, *108*, 4180–4186. (d) Savéant, J.-M. *Chem. Rev.* **2008**, *108*, 2348–2378. (e) Costentin, C.; Louault, C.; Robert, M.; Teillout, A.-L. *J. Phys. Chem. A* **2005**, *109*, 2984–2990.

(3) (a) Rondinini, S.; Mussini, P. R.; Crippa, F.; Sello, G. *Electrochem. Commun.* **2000**, *2*, 491–496. (b) Isse, A. A.; Gottardello, S.; Durante, C.; Gennaro, A. *Phys. Chem. Chem. Phys.* **2008**, *10*, 2409–2416.

(4) Isse, A. A.; Gottardello, S.; Maccato, C.; Gennaro, A. *Electrochem. Commun.* **2006**, *8*, 1707–1712.

(5) (a) Rondinini, S.; Mussini, P. R.; Muttini, P.; Sello, G. *Electrochim. Acta* **2001**, *46*, 3245–3258. (b) Falciola, L.; Gennaro, A.; Isse, A. A.; Mussini, P. R.; Rossi, M. *J. Electroanal. Chem.* **2006**, *593*, 47–56.

(6) (a) Isse, A. A.; De Giusti, A.; Gennaro, A.; Falciola, L.; Mussini, P. R. *Electrochim. Acta* **2006**, *51*, 4956–4964. (b) The phenomena reported in Figures 2 and 4 of ref 6a after long specific preconditioning of the silver cathode in the presence of benzyl chloride were not observed under our normal electrochemical conditions, with the voltammetric wave exhibiting pure diffusional behavior (peak current proportional to the square root of the scan rate). Furthermore, during our related SERS investigations 7 we did not observe any change of the adsorbed species detected along the foot of the wave even after the electrode has been poised during ca. 4 min at each sampled potential. This shows that though of interest under the specific conditions explored in ref 6a the phenomena reported in this reference are not active under our conditions.

at these electrodes has been the focus of several detailed electrochemical studies.[4,5] However, the exact origin of its remarkable properties has remained elusive, mostly because electrochemical information alone is not sufficient to delineate and ascertain quantitatively its mechanism.

In this connection, we recently reported that, during this reaction course, three unsuspected intermediates in close interaction with the silver cathode surface could be unraveled by *in situ* SERS (surface-enhanced Raman spectroscopy) investigations.[7] Though offering significant unsuspected entries in the mechanistic debate, SERS alone could not offer an unequivocal mechanistic framework to fully rationalize the electrocatalytic role played by silver surfaces. We wish to show that coupling DFT evaluations of the thermodynamic stabilities of the intermediates identified by SERS with quantitative voltammetric peak potential analysis allows a precise description of the main mechanistic features which sustain the exceptional electrocatalytic properties of silver cathodes. The mechanistic framework revealed in this work contrasts drastically with any of those tentatively invoked previously and shows that these exceptional electrocatalytic properties are a direct consequence of the electrophilicity of silver surface toward organic halides.

This work also provides evidence that the boundary between concerted and nonconcerted pathways in electrochemistry[2] is certainly more complex than what may be predicted upon considering only reactions at inert electrodes.

Results and Discussion

Delineation of the Main Mechanistic Framework. Let us briefly recall the well documented mechanism of $PhCH_2Cl$ reduction at inert electrodes like glassy carbon.[2,4,8] It involves a sequential pair of single-electron-transfers leading first to the 1e-concerted rupture of the carbon−chlorine bond (eq 1)[2] and then to the 1e-reduction of the free benzyl radical formed in solution (eq 2). This gives rise to a benzyl anion which spontaneously evolves to the final products (eq 4):[4,8]

$$PhCH_2Cl + e \rightarrow PhCH_2^{\bullet} + Cl^- \quad (rds),\ [(E^\circ{}_1)_{inert},\ k^\circ{}_{inert},\ E^p_{inert}] \qquad (1)$$

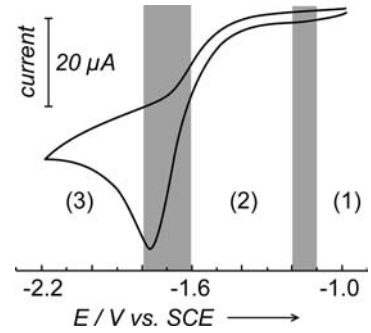

Figure 1. Cyclic voltammetry of $PhCH_2Cl$, 5 mM in 0.1 M TEAP + CH_3CN, at a Ag electrode (2 mm diameter) and a scan rate of 0.2 V s^{-1} ($E^p = -1.76$ V vs SCE). The three regions (1−3) represent potential ranges in which distinct intermediates were observed by SERS (see text);[7a] the gray ones represent zones where intermediates from adjacent zones coexist as evidenced by the overlap of their individual SERS spectra.

$$PhCH_2^{\bullet} + e \rightarrow PhCH_2^- \quad [E^\circ{}_2 > E^p_{inert}] \qquad (2)$$

$$PhCH_2^{\bullet} + \text{etc.} \quad (\text{negligible}) \qquad (3)$$

$$PhCH_2^- \rightarrow \text{etc.} \quad (\text{fast, see eqs } 5 - 8) \qquad (4)$$

Previous investigations of the mechanism in eqs 1−4 have pointed out that the whole electrochemical process is kinetically limited by the concerted electron-transfer step in eq 1[2] which acts as the rate-determining step (rds). Overall, the process is bielectronic,[8c] showing that the second reduction (eq 2) is fast at the potential of the voltammetric wave so there may not be any detectable interference by eq 3.[9] The nature and distribution of electrolysis products is characteristic of the spontaneous chemical evolution of a benzyl anion in slightly protic acetonitrile:[4,8c]

$$PhCH_2^- + CH_3CN \rightarrow PhCH_3 + {}^-CH_2CN \qquad (5)$$

$${}^-CH_2CN + PhCH_2Cl \rightarrow PhCH_2CH_2CN + Cl^- \qquad (6)$$

$$PhCH_2^- + PhCH_2Cl \rightarrow PhCH_2CH_2Ph + Cl^- \quad (\text{negligible}) \qquad (7)$$

$$PhCH_2^- + MH \rightarrow PhCH_3 + M^- \qquad (8)$$

Here, MH represents any other proton donor than acetonitrile, viz., residual water, supporting electrolyte, etc.

Voltammetric and electrolytic investigations at silver electrodes showed that these overall features remain essentially identical except for the drastic anodic shift of the voltammetric peak potential by 0.5 V (e.g., at $\upsilon = 0.2$ V s^{-1}: $E^p_{silver} = -1.76$ V versus SCE compared to $E^p_{inert} = -2.26$ V versus SCE as interpolated from ref 2a) irrespective of the scan rate since both peak-potential variations with $\log(\upsilon)$ and half-widths are identical. The voltammetric wave (see Figure 1) remains bielectronic[4,8c] and still exhibits a pure diffusional behavior controlled by slow charge-transfer kinetics ($\alpha = 0.3$).[4,10] These characteristic features establish that under our normal electrochemical conditions the electrocatalytic role of the silver cathode is not due to any strong alteration of the cathode surface as suggested to occur

(7) (a) Wang, A.; Huang, Y.-F.; Kumar Sur, U.; Wu, D.-Y.; Ren, B.; Rondinini, S.; Amatore, C.; Tian, Z.-Q. *J. Am. Chem. Soc.* **2010**, *132*, 9534–9536. (b) The rapid up-hill formation of a $PhCH_2Cl$ weak adduct onto the silver surface was indicated by (i) the weakness of its SERS spectrum intensity, (ii) the fact that its peak frequencies differed only modestly from those of a free benzyl chloride, and (iii) the constancy of this signal with time all along the foot of the voltammetric wave.[7a]

(8) (a) Isse, A. A.; Falciola, L.; Mussini, P. R.; Gennaro, A. *Chem. Commun.* **2006**, 344–346. (b) Wipf, D. O.; Wightman, R. M. *J. Phys. Chem.* **1989**, *93*, 4286–4291. (c) In fact since the overall reduction involves 20% yield in 3-phenylpropanenitrile, a 1e-product, the electron stoichiometry is 1.8 F/mol; yet by convenience, as previous authors, we use the formulation "bi-electronic" to recall that the mechanism is essentially bi-electronic, with 3-phenylpropanenitrile being formed by a follow-up reaction due to an S_N2 reaction of the $^-CH_2CN$ anion (formed during protonation of $PhCH_2^-$ by the acetonitrile solvent) onto the parent benzyl chloride. The same is true at silver cathodes since 3-phenylpropanenitrile is obtained with the same 20% yield, so that we use the same convenient formulation. Note, however, that in both cases this cannot be detected on the basis of voltammetry alone in the absence of extreme precision on the electrode surface area and diffusion coefficient of benzyl chloride. (d) For a discussion about absolute measurement of electron stoichiometries in transient electrochemistry see the following: Amatore, C.; Azzabi, M.; Calas, P.; Jutand, A.; Lefrou, C.; Rollin, Y. *J. Electroanal. Chem.* **1990**, *288*, 45–63.

(9) Amatore, C.; Savéant, J.-M. *J. Electroanal. Chem.* **1981**, *123*, 203–217.

(10) Nadjo, L.; Savéant, J. M. *J. Electroanal. Chem.* **1973**, *48*, 113–145.

in ref 6a after specific preconditioning of the silver cathode or to 2D or 3D organic−metallic phases as reported by Simonet et al. for the reduction of organic halides at several electrode materials including noble metals and silver.[11]

The product distribution remains essentially identical to that observed at inert electrodes,[4,8c] strongly suggesting that it again results from the spontaneous evolution of a free benzyl anion (eqs 5−8).

Conversely, SERS investigations established that at silver cathodes the first reduction involves a benzyl chloride weakly adsorbed through interaction of its C−Cl bond with the silver surface (zone 1 of Figure 1).[7] As soon as a significant electrochemical current starts to flow (zone 2 of Figure 1) this signal disappears and is replaced by the superimposition of those of a bound benzyl radical and its corresponding benzyl anion adduct. The relative intensities of the anionic adduct characteristic bands vis-à-vis those of the neutral adduct increase when the potential is made more negative, indicating that the steady-state concentration ratio of the two adducts is displaced in favor of the anionic form. Both signals then progressively vanish at higher potentials and are replaced by those of the 3-phenylpropanenitrile/silver adduct (zone 3 of Figure 1). This species may arise only from a sequence of reactions akin to those in eqs 5 and 6.[8d] Since the product distribution and the yield of this species are essentially identical to those observed at inert electrodes, this suggests that most probably the anionic benzyl adduct dissociates at sufficiently negative potentials to afford a benzyl anion prone to proceed along eqs 5−8 as it does at inert electrodes. Due to the strong affinity of the silver surface for nitrile moieties,[7] 3-phenylpropanenitrile may then adsorb.

Hence, the SERS data are perfectly consistent with the identity of the product distributions observed at inert and silver cathodes, while providing evidence that at silver electrodes the mechanism proceeds through the crucial involvement of at least three unsuspected organometallic surface species characterized by their SERS signals.

$$PhCH_2Cl + Ag \rightarrow [PhCH_2Cl\cdots Ag] \quad \text{(up-hill pre-equilibrium)} \tag{9}$$

$$[PhCH_2Cl\cdots Ag] + e \rightarrow [PhCH_2\text{-}Ag] + Cl^- \quad \text{(concerted or sequential)} \tag{10}$$

$$[PhCH_2\text{-}Ag]^\bullet + e \rightarrow [PhCH_2\text{-}Ag]^- \tag{11}$$

$$[PhCH_2\text{-}Ag]^- \rightarrow PhCH_2^- + Ag \tag{12}$$

$$PhCH_2^- \rightarrow \text{etc.} \quad \text{(fast; see eqs 5 − 8)} \tag{13}$$

As established by Laviron,[12] the absence of any specific voltammetric alterations, i.e., as expected when strongly adsorbed intermediates are involved,[13a] is not contradictory with the SERS observation that the first reduction proceeds through a weak adduct of benzyl chloride onto the silver surface (eq 9).[7b] Indeed, provided that this species is fleeting, it acts only as a transient precomplex formed before the very electron-transfer step in the very sense of the Debye−Schmoluchowski description of electron transfers.

The SERS observation of a benzyl radical−silver adduct as the first observable intermediate[7a] does not imply that this species is generated during the first elementary reduction step. It may only be the first 1e-intermediate which presents sufficient stability to be observable spectroscopically. Hence, at this stage, eq 10 should be viewed either as an elementary step (viz., a concerted one) or as the transient outcome of a sequential process. Similarly, though the reduction of the radical adduct into the anionic one in eq 11 is necessary to account for an overall bielectronic process,[8c] it is not yet determined if the change in reduction potential vis-à-vis that of a free benzyl radical into its free anion (eq 2)[14] allows such a step to proceed over the whole potential range where the voltammetric wave is displayed. Hence, the relative magnitude of the adsorption enthalpies of the adducts involved in eq 11 plays a crucial role in determining the feasibility of this step.

In the following we wish to establish that combining voltammetric data with thermodynamic ones predicted by DFT[15] for the different intermediates envisioned in reactions 9−11 allows us to answer the preceding two crucial mechanistic issues. This will finally serve to establish that the exceptional electrocatalytic properties of silver cathodes stem from the fact that they provide a mechanistic bridge between classical electrochemical activations of organic substrates and their organometallic counterparts.

Thermodynamic Evaluation of the Stability of Adducts in Reactions 9−11 by DFT. In our earlier contribution,[7a] DFT was used to predict the structures and SERS spectra of the different adducts considered above so as to identify them on the basis of the experimental SERS spectra. DFT may be also used to evaluate their thermodynamic stabilities relative to the unbound parent species. These are summarized in Table 1 on the basis of the DFT optimized structures of the adducts onto a Ag_4 cluster which was found to correctly represent a silver surface reactivity for our present purpose.[7a]

(11) (a) Simonet, J.; Peters, D. G. *J. Electrochem. Soc.* **2004**, *151*, D7–D12. (b) Simonet, J. *J. Electroanal. Chem.* **2005**, *583*, 34–45. (c) Simonet, J.; Poizot, P.; Laffont, L. *J. Electroanal. Chem.* **2006**, *591*, 19–26. (d) Simonet, J. *J. Electroanal. Chem.* **2006**, *593*, 3–14. (e) Ghilane, J.; Guilloux-Viry, M.; Lagrost, C.; Simonet, J.; Hapior, P. *J. Am. Chem. Soc.* **2007**, *129*, 6654–6661. (f) Poizot, P.; Laffont-Dantras, L.; Simonet, J. *Platinum Met. Rev.* **2008**, *52*, 84–95. (g) Poizot, P.; Laffont-Dantras, L.; Simonet, J. *J. Electroanal. Chem.* **2008**, *622*, 204–210. (h) Poizot, P.; Laffont-Dantras, L.; Simonet, J. *Electrochem. Commun.* **2008**, *10*, 864–867. (i) Poizot, P.; Laffont-Dantras, L.; Simonet, J. *J. Electroanal. Chem.* **2008**, *624*, 52–58. (j) Simonet, J. *J. Electroanal. Chem.* **2009**, *632*, 30–38. (k) Simonet, J. *Electrochem. Commun.* **2009**, *11*, 134–136. (l) Jouikov, V.; Poizot, P.; Simonet, J. *J. Electrochem. Soc.* **2009**, *156*, E171−E178. (m) Simonet, J. *J. Appl. Electrochem.* **2009**, *39*, 1625–1632. (n) Poizot, P.; Jouikov, V.; Simonet, J. *Tetrahedron Lett.* **2009**, *50*, 822–824. (o) Simonet, J. *J. Electrochem. Commun.* **2010**, *12*, 520–523. (p) Jouikov., V.; Simonet, J. *J. Electrochem. Commun.* **2010**, *12*, 331–334. (q) Jouikov, V.; Simonet, J. *Electrochem. Commun.* **2010**, *12*, 781–783.

(12) Laviron, E. *J. Electroanal. Chem.* **1995**, *382*, 111–127.

(13) Bard, A. J.; Faulkner, L. R. *Electrochemical Methods*; Wiley: New York, 1980; (a) pp 519−532; (b) p 223; (c) pp 443−451; (d) pp 454−455 and Figure 11.3.4 therein.

(14) The reduction potential of the benzyl radical in acetonitrile at a gold electrode has been reported to lie in between−1.43 and−1.45 V versus SCE. See the following:(a) Sim, B. A.; Milne, P. H.; Griller, D.; Wayner, D. D. M. *J. Am. Chem. Soc.* **1990**, *112*, 6635. (b) Grampp, G.; Muresanu, C.; Landgraf, S. *Electrochim. Acta* **2008**, *53*, 3149–3155.

(15) Frisch, M. J. et al. *Gaussian09*, revision A.02; Gaussian, Inc.: Wallingford, CT, 2009.

Table 1. Thermodynamic Energies of Adsorption on a Naked Ag_4 Cluster of the Different Moieties Considered in This Work As Deduced by DFT[a]

adduct	energy (kcal/mol.) ΔE	ΔH	ΔG
benzyl chloride-Ag_4	−3.6	−2.8	5.4
benzyl radical-Ag_4	−16.4	−16.0	−6.3
benzyl anion-Ag_4	−26.4	−26.1	−16.9
acetonitrile-Ag_4	−8.6	−7.9	−1.5

[a] See Supporting Information in ref 7 for the corresponding configurations and the coordinates of the models.

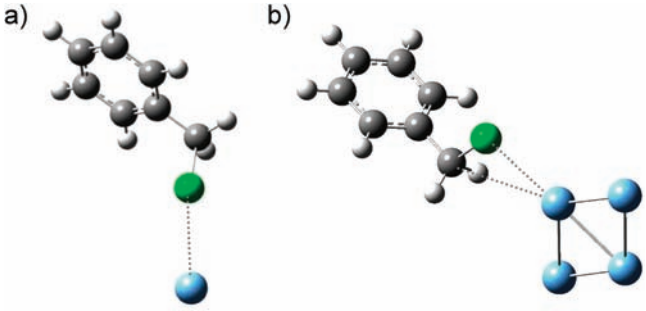

Figure 2. DFT optimized structures of adducts of benzyl chloride onto the silver surface as a function of the number of silver atoms used in modeling the silver surface: (a) Ag_1; (b) Ag_n, $n = 2-5$ and 10 (shown for $n = 4$).

Interestingly, Table 1 reports that the energy and enthalpy of formation of the benzyl chloride−silver adduct are weak but negative in agreement with the expected affinity of the silver surface for chlorine which was previously invoked as part of the electrocatalytic mechanism.[3−5,6a,8a] However, the ensuing Gibbs adsorption free energy results in a positive value (though still small), thus providing evidence of the constraints enforced into the organic frame during adsorption (compare Figure 2b). Such a small positive value of ΔG°_{ads} is perfectly consistent with regard to the weakness of the SERS intensity of the spectrum of the benzyl chloride adduct and the fact that its peak frequencies did differ only modestly from those of a free benzyl chloride molecule.[7]

To evaluate the role of the cluster size (Ag_n; $n = 4$ in Table 1) on the outcome of DFT-simulated thermodynamic quantities, the number of silver atoms was varied ($n = 1$ to 5 and 10). For $n = 2-5$ and 10, the structures of the adducts were consistently reproducible for the organic moiety as were the values of the predicted SERS bands and thermodynamic functions in vacuum. A four-atom cluster was thus preferred in the larger DFT simulations which incorporated also solvent contributions treated as a dielectric continuum (see also Experimental Section).

Conversely, for $n = 1$ drastic structural changes were observed in the adduct as shown for example by comparing the two structures predicted for the benzyl chloride precomplex in Figure 2. For the more realistic models ($n = 2-5$, 10) benzyl chloride was found to interact with one silver atom of the cluster through its C−Cl bond in a configuration strongly reminiscent of the first step of an oxidative addition.[16] This suggests that the neighbors of the interacting silver atom participate as ligands of a reactive metal center would do in a homogeneous organometallic oxidative addition.[16]

Table 1 also reports the adsorption energy of the acetonitrile solvent (ACN). Indeed, SERS revealed that the solvent may competitively adsorb at the electrode surface in zones 1 and 2 of Figure 1 (as well as the 3-phenylpropanenitrile end-product in zone 3).[7] Competitive adsorption of acetonitrile is then a parameter to be considered. For example, if one benzyl chloride displaces m ACN molecules, a better approximation of benzyl chloride Gibbs free energy of adsorption is $\Delta G^m_{ads} = \Delta G^{m=0}_{ads} - m(\Delta G^\circ_{ads})_{CH_3CN}$ where $\Delta G^{m=0}_{ads}$ is the value reported in Table 1 for $m = 0$. In any instance, since $(\Delta G^\circ_{ads})_{CH_3CN} < 0$, this makes preadsorption of benzyl chloride even more unfavorable than reported in Table 1 for $m = 0$. The same problem also exists for the two benzyl adducts. Yet, owing to the similar geometries of the two adducts (Figure 2), the numbers of ACN molecules displaced in each case must be equal, so that the value of m should not affect the change in driving forces between reactions 11 and 2.

Reduction of the Benzyl Radical−Silver Adduct. The feasibility of reducing the benzyl radical adduct into the anionic one (eq 11) over the whole potential range covered by the voltammetric wave (Figure 1) is a crucial point. This determines the theoretical possibility of accounting for the observation of an overall two-electron wave through this reaction.[8c] Indeed, the wave does not exhibit any feature characteristic of any change of electron stoichiometry while it unfolds (Figure 1).

Reduction of a free benzyl radical into its free anion (eq 2) is predicted to occur at $(E^\circ_2)_{inert} = -1.43$ V versus SCE in acetonitrile;[14] i.e., its driving force is almost null at the foot of the wave observed at silver cathodes (region 1 in Figure 1). Conversely, since the adsorption Gibbs free energy of the benzyl anion is stronger than that of the neutral species (Table 1), reaction 11 is thermodynamically favored versus that in eq 2: $(E^\circ_2)_{silver} = (E^\circ_2)_{inert} + (\Delta G^\circ_{ads,radical} - \Delta G^\circ_{ads,anion})/F > (E^\circ_2)_{inert}$ where $\Delta G^\circ_{ads,radical}$ and $\Delta G^\circ_{ads,anion}$ are the adsorption Gibbs free energies of the benzyl radical and the benzyl anion, respectively (Table 1). Using the data in Table 1, one obtains $(E^\circ_2)_{silver} =$

(16) (a) For quantitative kinetic discussions about oxidative addition mechanistic pathways in homogeneous organometallic catalysis, see the following, e.g.: Amatore, C.; Jutand, A. In *Handbook of OrganoPalladium Chemistry for Organic Synthesis*; Negishi, E. I., Ed.; Wiley, New York, 2002; chapter III.2.19, pp 943−972. (b) For an evaluation of electron-transfer pathways in organometallic oxidative additions, see the following, e.g.: Amatore, C.; Pflüger, F. *Organometallics* **1990**, *9*, 2276–2282, and references therein. (c) For the importance of precomplexation during oxidative additions, see the following, e.g.: Amatore, C.; Azzabi, M.; Jutand, A. *J. Am. Chem. Soc.* **1991**, *113*, 1670–1677. For a general review on homogeneous versus heterogeneous organometallic catalysis in the context of palladium catalysis, see the following, e.g.: Phan, N. T. S.; Van Der Sluys, M.; Jones, C. W. *Adv. Synth. Catal.* **2006**, *348*, 609–679.

(17) (a) Marcus, R. A. *J. Chem. Phys.* **1965**, *43*, 679–701. (b) All electron-transfers considered in this work do not obey the requirement of Marcus theory for outer-sphere electron-transfers, although this does not prevent using Marcus formulations for reorganization energies for the sake of comparison to the experimental values determined. (c) Similarly, we resort to quadratic correlations between activation barriers and driving force (eq 19) without implying that the conditions of application of Marcus theory are obeyed since we do not evaluate the coefficient of the quadratic correlations based on Marcus expression of the intrinsic barrier $\Delta G^{\ddagger}_0$ but determine them experimentally. Quadratic correlations between activation barriers and driving force (eq 19) are much more general than the classical Marcus expression for outer-sphere electron-transfers and stem only from the geometric properties of the intersection of two potential wells whatever their shape and origin. In this respect, it must be pointed out that Marcus' major contribution was not to introduce such quadratic relationships which were pre-existing (for a discussion see refs 18a, d) but, importantly, to establish ab initio the fundamental origin of these linear and quadratic correlations in the particular case of outer-sphere electron-transfers. This led Marcus to demonstrate (1) the possibility of evaluating $\Delta G^{\ddagger}_0$ based on spectroscopic, structural, and thermodynamic physicochemical data, or from isotopic reactions (Marcus' cross-relationship), and (2) that an inverted region appears when $|\Delta G^\circ| > 4\Delta G^{\ddagger}_0$ provided that the product system has almost no vibronically excited states.

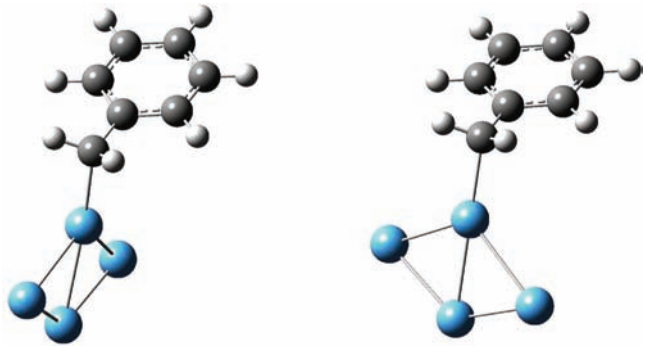

Figure 3. DFT optimized structures of the benzyl radical (left) and benzyl anion (right) adducts on a Ag_4 cluster.

$(E^\circ_2)_{inert} + 0.46$ V, i.e., $(E^\circ_2)_{silver} \approx -0.97$ V versus SCE. Such a value is amply sufficient for the reduction in eq 11 to be thermodynamically driven all along the voltammetric wave, including its very foot (region 1 in Figure 1). Nonetheless, such thermodynamic argument alone is not sufficient to prove the case, so let us examine now its feasibility from a kinetics point of view.

In the absence of any kinetics information, this issue may only be evaluated by comparison to the case of the outer-sphere reduction in eq 2 since this is known to proceed fast at inert electrodes.[2a] In this respect it is interesting to consider the charge distribution within the benzyl radical adduct as it is predicted by DFT, e.g., for Ag_4 (eq 14):

$$PhCH_2^\bullet + Ag_4 \rightarrow [PhCH_2^{-0.14} - Ag_4^{+0.14}]^\bullet \qquad (14)$$

This shows that in its neutral adduct the benzyl moiety is already partially charged negatively so that the outer-sphere reorganization occurring during the reduction in eq 11 is certainly less than that in eq 2. Hence, its outer-sphere reorganization energy, λ_o*,[17a] is certainly much smaller than that in eq 2. The same is true for the inner-sphere reorganization energy, λ_i*,[17a] since in the neutral state of the adduct the benzylic carbon is already hybridized in sp^3 as it is in the anionic adduct (Figure 3). Conversely, this hybridization must drastically change when a free benzyl radical (sp^2) is reduced into a free anion (sp^3) as in eq 2. This is evidence that the intrinsic activation barrier of reaction 11 is much less than that of the reduction of a free benzyl radical. Hence, one may safely conclude that the reduction in eq 11 is feasible both thermodynamically and kinetically over the whole potential range of the voltammetric wave observed at silver cathodes (Figure 1).

To conclude this section, another kinetic possibility needs to be considered. This would involve a squared-scheme reduction of the neutral benzyl adduct: predesorption of the benzyl radical, followed by its reduction in solution and binding of the ensuing free anion in competition with its fast spontaneous chemical reactions in eqs 5−8. Yet in this case, the uphill desorption would disfavor the overall reduction by +6.3 kcal/mol (Table 1), i.e., by ca. 0.27 V. Since $(E^\circ_2)_{inert} = -1.43$ V versus SCE for the free radical,[14] the apparent standard reduction potential for this route would be ca. −1.70 V. This shows that such a pathway is thermodynamically hampered over most of the potential range of interest and could not account for the observation of a full-fledged bielectronic wave.[8c] It may then be safely concluded that the second reduction step occurs between the benzyl adducts as represented in eq 11.

Our previous SERS investigations[7a] revealed that at sufficiently negative potentials (region 3 in Figure 1) the anionic adduct signal disappears and is replaced by that of the adsorbed 3-phenylpropanenitrile product. One may argue that this stems from the chemical reactivity of the adduct as such. Yet owing to the close identity between the product distributions at inert and silver cathodes, one is inclined to believe that the final steps occur from a dissociated benzyl anion (eqs 5−8) and that the 3-phenylpropanenitrile adduct is formed by adsorption of the nitrile product after its formation in solution. Dissociation of the benzyl anion is certainly enforced by the growing electrostatic repulsion[13a] exerted by the increasingly negative electrode potential onto the negatively charged adsorbed organic moiety (compare to eq 14 for the radical adduct). Note that the same electrostatic factor certainly explains why no adsorption of chloride ion, a necessary product of reaction 10, could be observed by SERS over the potential range of the voltammetric wave[7] despite the affinity of chloride ions for silver surfaces.

General Considerations about the Mechanism of the First Reduction Step. SERS investigations established that at silver electrodes benzyl chloride reduction begins through an electron transfer onto its weakly bound surface complex to provide, directly or sequentially, a bound benzyl radical. The above section confirmed that such benzyl adduct could then be easily reduced so as to lead to an overall bielectronic voltammetric wave. This also implies that the fact that signals are observed for both benzyl adducts is due to kinetics, with the surface concentration of the neutral species obeying a dynamic steady state between its formation (eq 10) and its reduction (eq 11) in which the former decreases while the wave is spanned due to decreasing diffusion rate of the benzyl chloride to the electrode while the latter increases with the increasingly negative potential of the electrode. This is coherent with the progressive decrease of the neutral benzyl adduct contribution while the wave is spanned.

Hence, this weak adsorption necessarily acts as an uphill preceding step to the electron-transfer one (CE mechanism).[13c] Under such conditions[12] no usual voltammetric features related to adsorption[13a] may be observed in agreement with the pure diffusional appearance of the wave in Figure 1. Scheme 1 illustrates the different mechanistic possibilities which are consistent with the SERS observations and which may link mechanistically the benzyl chloride precomplex to the first intermediate identified by SERS.

On the basis of our best knowledge, Scheme 1 considers all the possible situations which are consistent with present electroorganic views. These are classified into two categories depending on the concerted or nonconcerted nature of the elementary electron-transfer step. Note that, except for the absence of a chloride ion adsorption which did not occur based on the absence of the characteristic Ag−Cl features in the SERS spectra,[7a] the concerted pathways I summarize all those which have been tentatively considered in previous works to account for the strong electrocatalytic effect of silver cathodes. To our best knowledge, the nonconcerted pathways II have never been considered. For this reason, in the following, we consider all pathways summarized in Scheme 1 without any preconsideration about their occurrence.

In the first concerted possibility (case I-1), the reduction of the initial adduct would give rise to a free benzyl radical such as that formed at inert electrodes. In this case the electron transfer would be concerted with the rupture of the weak binding of the substrate as well as with the rupture of the comparatively

Scheme 1

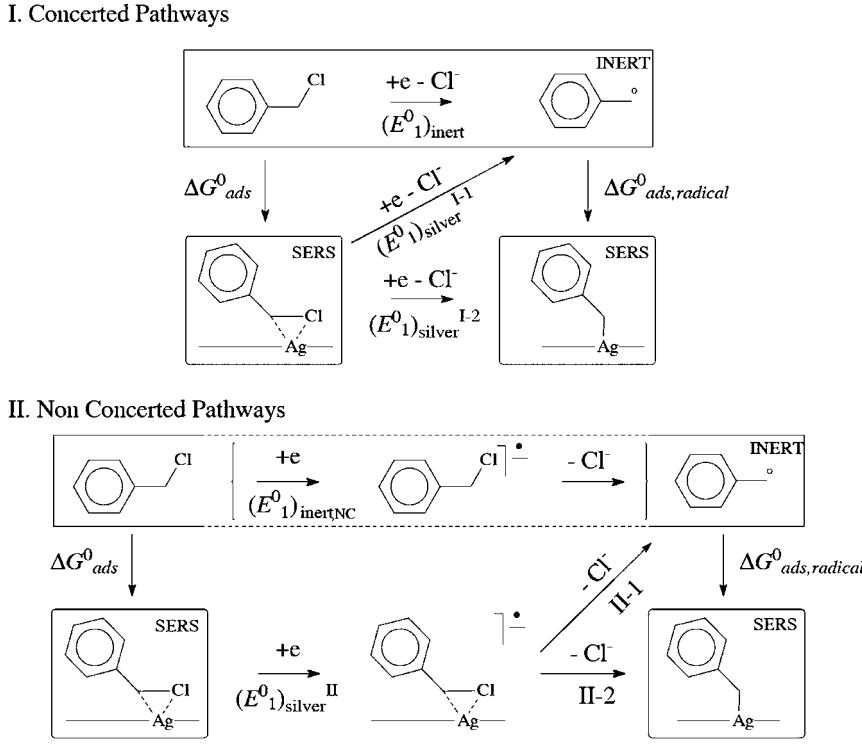

stronger carbon−chlorine bond. This step would then be favored thermodynamically but disfavored kinetically versus that in eq 1. Indeed, if the uphill precomplexation favors thermodynamically the electron-transfer step, it burdens its activation barrier since only a fraction $\alpha \approx 0.3$ of this gain may help to reduce the electron-transfer barrier. Furthermore, within the framework of concerted electron transfers, involving an additional structural contribution (vs that in eq 1) in a concerted step should result in a larger intrinsic activation barrier.[2a] Hence, it appears doubtful that mechanism I-1 may outrun that observed at an inert electrode (eq 1). One cannot conclude so easily about the occurrence of mechanism I-2. Indeed, here the electron-transfer step involves in addition a concerted binding of the benzylic carbon onto the silver surface. This may look awkward within an electrochemical framework, but this is an exact heterogeneous mechanistic analogue of homogeneous oxidative additions during which a weakly coordinated carbon−halogen bond is reductively cleaved while each moiety binds to the metal center.[16] Yet, such a step is expected to have an even larger intrinsic activation barrier than that in case I-1 due to an additional contribution due to the creation of the carbon−benzyl bond. Indeed, even if this bond is already prefigured in the $PhCH_2Cl$−Ag adduct (compare Figure 2b), its elongation and its weakness provide evidence that it is far from the strong bond ultimately present in the benzyl−Ag adduct. Conversely, it would be highly favored thermodynamically compared to case I-1 and to the concerted reaction 1 due to the large stabilization of its product, a gain which also contributes to a decrease of the effective activation barrier of the CE sequence. Hence, without any quantitative evaluation of each effect, one cannot conclude about the overall ability of route I-2 in outrunning the simple concerted mechanism in eq 1.

Within the nonconcerted mechanistic set II, a 1e-intermediate on the way between an anion radical and the fully dissociated pair, $PhCH_2^{\bullet} + Cl^-$,[2a] is envisioned as a possible primary product of the first electron transfer, its hypothetical transient existence being ascribed to a stabilization through a close interaction with the silver surface. This hypothetical species may then evolve directly to the benzyl radical−silver adduct (case II-2) or dissociate to generate a free benzyl radical which then may adsorb onto the cathode surface (case II-1) in competition with its reduction.[9]

At inert electrodes, electrochemical reduction of benzyl chloride may not proceed through the corresponding anion radical due to the highly negative value of $(E°_1)_{inert,NC}$ in Scheme 1.[2a] This has indeed been evaluated to be at least −2.9 V versus SCE,[2a] while $(E°_1)_{inert} = -0.76$ V versus SCE[2a] for the concerted electron transfer in eq 1. Yet, the concerted process has a much higher intrinsic activation barrier, $(\Delta G^{\ddagger}_0)_{inert} = 20.7$ kcal/mol,[2a] than that, $(\Delta G^{\ddagger}_0)_{inert,NC} \approx 4.5$ kcal/mol, of the would-be formation of a free anion radical as follows from Marcus' expression of the corresponding outer-sphere reorganization energy.[17a] The important inner reorganization energy of the concerted pathway (eq 1) explains why the reduction wave of benzyl chloride at inert electrodes is observed at considerably more negative potentials (−2.26 V vs SCE at 0.2 V s^{-1} as interpolated from ref 2a) than its standard potential. In this respect it is inferred that if $(\Delta G^{\ddagger}_0)_{inert}$ was larger, the concerted process would not be able to compete with the nonconcerted one for kinetic reasons though it would remain highly favored thermodynamically.

Though not generally expressed in this way, this shows that competition between concerted and nonconcerted mechanisms is between a kinetically easy but thermodynamically difficult route (nonconcerted) versus a kinetically difficult but thermodynamically favored one (concerted). Hence, any effect that would stabilize sufficiently an anion radical intermediate without increasing too much the corresponding reorganization energy may well lead to a situation in which the formation of such an intermediate would outrun the concerted pathway. In this respect, it is worth noticing that we have shown above that silver cathode surfaces may donate (benzyl chloride precomplex,

benzyl radical adduct) or accept (benzyl anion adduct) electron density in a similar way as an organometallic center proceeds during the activation of organic halides.[16] Hence it is not unreasonable to envision that similar electronic effects may contribute to stabilize a complexed anion radical through stabilizing the $\pi/\pi^*-\sigma/\sigma^*$ coupled organic orbitals by partial donation to the silver cathode. If the carbon−chlorine bond in such an intermediate is sufficiently elongated though not cleaved, the energetic demand of its formation may then be drastically decreased vis-à-vis that required to create a free anion radical while not severely burdening the intrinsic electron-transfer activation barrier. At least at this general hypothetical level, this justifies considering the hypothetical occurrence of the nonconcerted pathways in Scheme 1.

In the following, we wish to evaluate quantitatively the information concealed in the voltammetric peak potentials of the waves observed at inert electrodes and silver cathodes and contrast them to the DFT predictions concerning the intermediates observed by SERS to examine if this allows discriminating among the four pathways represented in Scheme 1.

Quantitative Considerations about the First Reduction Mechanism. To proceed further, we need first to recall several basic but crucial features attached to irreversible voltammetric waves (viz., controlled by overall slow charge-transfer kinetics)[10,13b] since they are essential to the following analysis. Indeed, even if these are present in textbooks, they are often improperly used.

Fully irreversible voltammetric waves are controlled by the interplay between diffusion, thermodynamics, and the corresponding heterogeneous rate law. The latter may be expressed as follows for all the cases at hand (Scheme 1 and eq 1), irrespective of the exact mechanism involved:[10,13b]

$$I = -FADk[\mathrm{PhCH_2Cl}]_0 \qquad (15)$$

Here I is the voltammetric current, A the electrode surface area, D the diffusion coefficient of the benzyl chloride substrate, k the effective heterogeneous rate constant at the electrode potential E under consideration (k°, the standard rate constant, is the value of k at $E = E^\circ$), and $[\mathrm{PhCH_2Cl}]_0$ the free benzyl chloride concentration in solution at angstrom distances from the electrode surface, i.e., just before interacting with the very electrode surface. Note that the use of an irreversible electron transfer rate law in eq 15 does not imply necessarily that the backward rate constant is negligible. This may apply also when the first reaction product is highly unstable since then the overall kinetics of electron transfer may only proceed in the forward direction.[10,13d]

The heterogeneous rate constant k varies with the driving force $F(E - E^\circ)$ via the dependence of its effective activation barrier $(\Delta G^\ddagger)_{\mathrm{eff}}$ on this parameter:[18,19]

$$k = \kappa Z \exp[-(\Delta G^\ddagger)_{\mathrm{eff}}/RT] \qquad (16)$$

Here κ is the adiabatic transmission factor (in the following we consider that $\kappa = 1$ as usual for electrochemical reactions due to the high quantum coupling between the substrate and the metal)[2a,18e,f] and $Z = (RT/2\pi M)^{1/2}$ (where M is the molar mass of $\mathrm{PhCH_2Cl}$, i.e., $Z = 5.6 \times 10^3$ cm s^{-1}). When there is a direct reduction of the substrate as occurs at inert electrodes, $(\Delta G^\ddagger)_{\mathrm{eff}}$ is the activation barrier of the electron-transfer elementary step (E) whatever its intrinsic nature (viz., concerted or not): $(\Delta G^\ddagger)_{\mathrm{eff}} = (\Delta G^\ddagger)_{\mathrm{E}}$. Conversely, within a CE sequence controlled kinetically by the electron-transfer step,[12,13c] i.e., when the chemical step (C) has a positive Gibbs free energy, $(\Delta G^\circ)_{\mathrm{C}}$, the pre-equilibrium free energy acts as a "work" term in Debye−Schmoluchovski theory:[18a−d] $(\Delta G^\ddagger)_{\mathrm{eff}} = (\Delta G^\ddagger)_{\mathrm{E}} + (\Delta G^\circ)_{\mathrm{C}}$. In Scheme 1, the uphill pre-equilibrium step consists of the adsorption of benzyl chloride onto the silver cathode surface,[12] so that $(\Delta G^\circ)_{\mathrm{C}} = \Delta G^\circ_{\mathrm{ads}}$ where $\Delta G^\circ_{\mathrm{ads}}$ is the adsorption Gibbs free energy of the benzyl chloride onto the silver surface (Table 1). Hence, eq 16 is rewritten as follows for each type of electrode material. At inert electrodes (eq 1)

$$k^{\mathrm{inert}} = Z \exp[-(\Delta G^\ddagger)_{\mathrm{E,inert}}/RT] \qquad (17)$$

and

$$k^{\mathrm{silver}} = Z \exp\{-[(\Delta G^\ddagger)_{\mathrm{E,silver}} + \Delta G^\circ_{\mathrm{ads}}]/RT\} \qquad (18)$$

at silver electrodes (Scheme 1), irrespective of the exact mechanism followed.

Savéant et al. established that, irrespective of the exact type of electron transfer considered (viz., concerted or not),[2a,d,e] the dependence of $(\Delta G^\ddagger)_{\mathrm{E}}$ on the electrode potential, i.e., with $F(E - E^\circ)$,[19] may always be formulated within a Marcusian framework. The exact nature of the electron-transfer step (concerted or not) is then only reflected by the value of its standard potential E° and by its intrinsic activation barrier $\Delta G^\ddagger_0$ (viz., the value of $(\Delta G^\ddagger)_{\mathrm{E}}$ at $E = E^\circ$). Thus, irrespective of the situation considered, $(\Delta G^\ddagger)_{\mathrm{E}}$ in eqs 17 or 18 is given by[2a,17b,c,19]

(18) (a) Amatore, C. In *Organic Electrochemistry*; Lund, H., Hammerich, O., Eds.; M. Dekker: New York, 2000; chapter 1, p 61 and the following pages. For discussions about the reasons justifying the combination of "work terms" in the "effective" activation barrier, see. (b) ref 17a. (c) Marcus, R. A. *Discuss. Faraday Soc.* **1960**, *129*, 21. (d) Schlesener, C. J.; Amatore, C.; Kochi, J. K. *J. Phys. Chem.* **1986**, *90*, 37473756. These two latest works consider bimolecular homogeneous reactions, but the concepts involved are readily transposable to heterogeneous cases within the Marcus framework (upon considering the electrode as one infinite reactant plane). For a discussion of this latter point, see the following reference. (e) Kojima, H.; Bard, A. J. *J. Am. Chem. Soc.* **1975**, *97*, 63176324. Yet the metallic nature of the electrode introduces some electrostatic mirror effects not accounted for in bimolecular cases. See the following reference. (f) Hale, J. M. In *Reactions of Molecules at Electrodes*; Hush, N. S., Ed.; Wiley Interscience: New York, 1971, chapter 4, p 229.

(19) To be rigorous, the electrode potential E in eq 24 should be replaced by the expression $(E-\phi)$ where ϕ is the Frumkin double-layer potential term which accounts for the fact that the electron-transfer site is not located at the very surface of the electrode (where E prevails) but a few angstroms from it, in proximity to the outer Helmholtz plane (OHP), where the effective potential is $E-\phi$. Yet, under most circumstances the site of electron transfer is not known with sufficient precision so that ϕ is unknown, especially at solid polycrystalline electrodes and in organic solvents. Furthermore, this value is also modified by electrostatic mirror effects due to the metallic surface of the electrode which acts on the kinetics (see refs 18e, f). Therefore, this term is generally not accounted for, the ensuing error being then shuttled into the experimental $\Delta G^\ddagger(E)$ value, i.e., somewhat corrupting the exact meaning of the determined value of $\Delta G^\ddagger_0$.

(20) This relationship may appear surprising at first glance but should be readily understood; the observation of a CV wave at a given scan rate (i.e., of a current flow compatible with a diffusion-limited supply at this scan rate) requires that the electron-transfer rate constant has the exact magnitude required for sustaining this precise current flow (compare eq 15). This condition may be fulfilled only when the potential-dependent effective activation barrier at the CV peak potential reaches a constant magnitude (compare eq 22) irrespective of the exact elementary steps under voltammetric scrutiny.

$$(\Delta G^{\ddagger})_{E} = \Delta G^{\ddagger}_{0} \times [1 + F(E - E^{\circ})/4\Delta G^{\ddagger}_{0}]^{2} \quad (19)$$

though the values of E° and $\Delta G^{\ddagger}_{0}$ depend on the exact case at hand and the latter does not necessarily obey Marcus' classical expression since the present electron-transfers do not obey the outer-sphere requirements.[17b,c]

Under most experimental circumstances the potential range in which the voltammetric wave may be observable is small enough versus $\Delta G^{\ddagger}_{0}/F$ that eq 19 may be approximated by its most usual Butler−Volmer formulation.[13b] This follows from a local linearization of its squared bracketed term

$$(\Delta G^{\ddagger})_{E} = \Delta G^{\ddagger}_{0} + \alpha \times F(E - E^{\circ}) \quad (20)$$

where α, the transfer coefficient, is then the mean value of

$$\alpha = [1 + F(E - E^{\circ})/4\Delta G^{\ddagger}_{0}]/2 \quad (21)$$

over the whole potential range spanned by a voltammetric wave for the scan rates, ν, of interest. On the basis of these definitions, one readily establishes that, at any given scan rate $(\Delta G^{\ddagger})_{eff}{}^{p}$, the value taken by $(\Delta G^{\ddagger})_{eff}$ at the voltammetric peak potential of any irreversible wave under slow charge control is given by[2a,13b]

$$(\Delta G^{\ddagger})^{p}_{eff} = RT(\ln Z - 0.78) + 0.5 \ln(RT/\alpha F\nu D) \quad (22)$$

for any values of E° and $\Delta G^{\ddagger}_{0}$, in eq 20 $\alpha \approx 0.3$ is experimentally determined to be approximately equal at silver electrodes and inert ones, and Z or D are by definition identical in each situation. Hence, eq 22 establishes that, irrespective of the exact mechanism followed, the values of $(\Delta G^{\ddagger})_{eff}{}^{p}$ observed for a given scan rate at each electrode material are equal. Note, however, that this identity relates two $(\Delta G^{\ddagger})_{eff}$ values which pertain to different E°, $\Delta G^{\ddagger}_{0}$, and different peak potentials ($\Delta E^{p} = E^{p}_{silver} - E^{p}_{inert} = 0.5$ V). Rewriting this relationship within the framework of eq 20 shows that at any given scan rate

$$(\Delta G^{\ddagger}_{0})_{silver} + \alpha F(E^{p} - E^{\circ}{}_{1})_{silver} + \Delta G^{\circ}_{ads} = (\Delta G^{\ddagger}_{0})_{inert} + \alpha F(E^{p} - E^{0}_{1})_{inert} \quad (23)$$

Since $\alpha \approx 0.3$ for both electrode materials (i.e., $\Delta E^{p} = E^{p}{}_{silver} - E^{p}{}_{inert}$ is constant), eq 23 may finally be rearranged to afford a linear equation relating $(\Delta G^{\ddagger}{}_{0})_{silver}$ and $(E^{\circ}{}_{1})_{silver}$:

$$(\Delta G^{\ddagger}_{0})_{silver} - \alpha F(E^{\circ}{}_{1})_{silver} = (\Delta G^{\ddagger}_{0})_{inert} - \Delta G^{\circ}{}_{ads} - \alpha F(E^{\circ}{}_{1})_{inert} - \alpha F\Delta E^{p} \quad (24)$$

in which all the right-hand terms are known. Note that, since this equation follows only from the properties of irreversible voltammetric waves (viz., from eq 22), it is independent of the specific mechanism (Scheme 1) underlying the values of $(\Delta G^{\ddagger}{}_{0})_{silver}$ and $(E^{\circ}{}_{1})_{silver}$.

A second relationship between these two parameters, again independent of the exact mechanism involved, is provided by recalling that $\alpha \approx 0.3$ is experimentally determined at each type of electrode. From eq 21 it then follows that at any scan rate of interest in this work

$$(E^{p} - E^{\circ}{}_{1})_{silver}/(\Delta G^{\ddagger}_{0})_{silver} = (E^{p} - E^{\circ}{}_{1})_{inert}/(\Delta G^{\ddagger}_{0})_{inert} \quad (25)$$

With a minimal value for $\Delta G^{\circ}{}_{ads} = 5.4$ kcal/mol (viz., upon neglecting the desorption of acetonitrile molecules, see above), and with the values of $(\Delta G^{\ddagger}{}_{0})_{inert}$,[2a] $(E^{\circ}{}_{1})_{inert} = -0.76$ V,[2a] $(E^{p})_{inert} = -2.26$ V,[2a] and $(E^{p})_{silver} = -1.76$ V versus SCE at 0.2 V s^{-1} as well as $\alpha = 0.3$, the solution of the linear two-equation−two-unknown system in eqs 24 and 25 affords $(\Delta G^{\ddagger}{}_{0})_{silver} = 10$ kcal/mol and $(E^{\circ}{}_{1})_{silver} = -1.0$ V versus SCE. These results are independent of the exact mechanism considered here. They only depend on the value of $\Delta G^{\circ}{}_{ads}$ which has been used and on the other independently known parameter or experimental data values. Note that as discussed before we used the minimum value of $\Delta G^{\circ}{}_{ads}$. Increasing $\Delta G^{\circ}{}_{ads}$ would lead to an even more negative value for $(E^{\circ}{}_{1})_{silver}$.[21] So $(E^{\circ}{}_{1})_{silver} = -1.0$ V versus SCE is the most positive value of $(E^{\circ}{}_{1})_{silver}$ consistent with the voltammetric observations and previously published data.[2a]

Then $(E^{\circ}{}_{1})_{silver}$ is found to be at least 0.24 V more negative than $(E^{\circ}{}_{1})_{inert}$. This result is clearly inconsistent with any of the concerted pathways envisioned in mechanisms I since by construction each of them should correspond to a decrease of the Gibbs free energy of the electron transfer due to the thermodynamic contribution of the uphill preadsorption step (route I-1) and of the cumulative effects of this step and of the formation of a stable benzyl radical−silver adduct (Table 1)

(21) In the main text the solution of the 2-equation linear system consisting of eqs 24 and 25 was searched in the most general case (viz., being valid for either paths I or II) in terms of the values of $(\Delta G^{\ddagger}{}_{0})_{silver}$ and $(E^{\circ}{}_{1})_{silver}$ while imposing $\Delta G^{\circ}{}_{ads}$ at its minimal value reported in Table 1 (see the corresponding discussion in text). However, if one restricts the analysis to the two mechanisms I-1 and I-2 a more simple solution may be proposed since this does not require fixing an a priori value for $\Delta G^{\circ}{}_{ads}$. Indeed, considering the thermodynamic cycles in Scheme 1, $(E^{\circ}{}_{1})_{silver}$ is a direct function of $(E^{\circ}{}_{1})_{inert}$ and $\Delta G^{\circ}{}_{ads}$ (mechanism I-1) or of $(E^{\circ}{}_{1})_{inert}$, $\Delta G^{\circ}{}_{ads}$, and $\Delta G^{\circ}{}_{ads,radical}$ (mechanism I-2):

$$(E^{\circ}{}_{1})^{I-1}_{silver} = (E^{\circ}{}_{1})_{inert} + \Delta G^{\circ}{}_{ads}/F \quad (\text{mechanism I} - 1) \quad (\text{FTN-1a})$$

$$(E^{\circ}{}_{1})^{I-2}_{silver} = (E^{\circ}{}_{1})_{inert} + (\Delta G^{\circ}{}_{ads} - \Delta G^{\circ}{}_{ads,radical})/F \quad (\text{mechanism I} - 2) \quad (\text{FTN-1b})$$

Equations FTN-1a,b may be rewritten into a unified form by introducing a parameter, ρ, defined such as $\rho = 0$ for mechanism I-1 and $\rho = -\Delta G^{\circ}{}_{ads,radical}/\Delta G^{\circ}{}_{ads}$ for mechanism I-2. Then

$$(E^{\circ}{}_{1})^{I}_{silver} = (E^{\circ}{}_{1})_{inert} + (1 + \rho)\Delta G^{\circ}{}_{ads}/F \quad (\text{mechanism I-1 or I-2}) \quad (\text{FTN-2})$$

so that eqn 24 becomes

$$(\Delta G^{\ddagger}_{0})_{silver} + [1 - \alpha(1 + \rho)]\Delta G^{\circ}{}_{ads} = (\Delta G^{\ddagger}_{0})_{inert} - \alpha F\Delta E^{p} \quad (\text{FTN-3})$$

Considering the numerical values $(E^{p})_{silver} = (E^{p})_{inert} + 0.5$ V, $(\Delta G^{\ddagger}{}_{0})_{inert} = 20.7$ kcal/mol,[2a] $(E^{\circ}{}_{1})_{inert} = -0.76$ V versus SCE,[2a] $(E^{p})_{inert} = -2.26$ V versus SCE at 0.2 V s^{-1},[2a] and $\alpha = 0.3$, eq FTN-3 becomes

$$(\Delta G^{\ddagger}_{0})_{silver} + (0.7 - 0.3\rho)\Delta G^{\circ}{}_{ads} = 17.2 \text{ kcal/mol} \quad (\text{FTN-4})$$

A second linear relationship between $(\Delta G^{\ddagger}{}_{0})_{silver}$ and $\Delta G^{\circ}{}_{ads}$ is given by rewriting eq 25 using the same procedure:

$$(\Delta G^{\ddagger}_{0})_{silver} - 0.6(1 + \rho)\Delta G^{\circ}{}_{ads} = 13.8 \text{ kcal/mol} \quad (\text{FTN-5})$$

Solution of the two-equation−two-unknown linear system in eqs FTN-4, FTN-5 affords $\Delta G_{ads} = 2.6$ kcal/mol for mechanism I-1 and $\Delta G^{\circ}{}_{ads} = (2.6 + 0.23\Delta G^{\circ}{}_{ads,radical})$ kcal/mol for mechanism I-2. Since $\Delta G^{\circ}{}_{ads,radical}$ is necessarily negative (Table 1), this result means that $\Delta G^{\circ}{}_{ads}$ needs to be lower than 2.6 kcal/mol for mechanism I-2 (note that using $\Delta G^{\circ}{}_{ads,radical} = 6.3$ kcal/mol (Table 1) would afford $\Delta G^{\circ}{}_{ads} = 1.15$ kcal/mol). Since the value of $\Delta G^{\circ}{}_{ads} = 5.4$ kcal/mol reported in Table 1 is the minimum one, both results cannot be reconciled with the present DFT thermodynamic evaluations and with the SERS evidence. This definitively rules out both concerted mechanisms I.

for route I-2. Hence, in both situations $(E°_1)_{silver}$ should be less negative than $(E°_1)_{inert}$. More precisely, since 5.4 kcal/mol is the minimal value of $\Delta G°_{ads}$, the thermodynamic cycle for mechanism I-1 in Scheme 1 predicts $(E°_1)_{silver}^{I-1} = (E°_1)_{inert} + \Delta G°_{ads}/F \geq -0.53$ V versus SCE. The outcome is even worse for mechanism I-2 since the formation of a stable bound benzyl radical (−6.3 kcal/mol, Table 1) necessarily corresponds to a much more positive value: $(E°_1)_{silver}^{I-2} = (E°_1)_{inert} + (\Delta G°_{ads} - \Delta G°_{ads,radical})/F \geq -0.25$ V versus SCE. Therefore, unless other effects not envisioned here were to be involved, the two concerted mechanisms labeled I in Scheme 1 have to be rejected for not being able to account quantitatively for the magnitude of the voltammetric wave shift between inert and silver cathodes.

Let us now examine the nonconcerted mechanisms in Scheme 1. The value of $(E°_1)_{inert,NC}$, i.e., that corresponding to the formation of a free anion radical, has been evaluated at ca. −2.9 V versus SCE or more negative.[2a] Compared to $(E°_1)_{silver} = -1.0$ V versus SCE obtained above by taking into account that $(E°_1)_{silver}$ applies to the adsorbed benzyl chloride, this shows that the primary product of the first electron transfer is stabilized by ca. 38.5 kcal/mol or more vis-à-vis a free benzyl chloride anion radical (as depicted in brackets in Scheme 1). This appears to be totally excessive for a simple complexation of a classical benzyl chloride anion radical unless the carbon−chlorine bond is severely extended. Conversely, the difference between $(E°_1)_{silver}$ and $(E°_1)_{inert}$ shows that the primary product at silver electrodes is uphill by ca. 11 kcal/mol vis-à-vis a fully dissociated pair $PhCH_2^{\bullet} + Cl^-$. This represents only about one-fifth of the ca. 50 kcal/mol or more separating a free anion radical and a dissociated pair $PhCH_2^{\bullet} + Cl^-$.[2a] Hence, describing tentatively this hypothetical species as an adduct "$[PhCH_2 \cdots Cl]^{\bullet -}$/Ag", in which the carbon−chlorine bond is considerably extended but still not fully cleaved, rather than as a fully fledged anion radical interacting with the silver electrode surface does not appear unrealistic. Such species would be similar to those envisioned as transition states in homogeneous organometallic oxidative additions.[16b]

The much smaller intrinsic activation barrier $\Delta G^{\ddagger}_0$ obtained at silver electrodes (10 kcal/mol) versus that at inert ones (20.7 kcal/mol)[2a] is also compatible with a permanence of a carbon−chlorine bond in this primary intermediate. Indeed, for a nonconcerted reduction at inert electrodes, one would predict $(\Delta G^{\ddagger}_0)_{NC} \approx 4.5$ kcal/mol upon considering Marcus' expression for the outer-sphere reorganization energy.[17a] Hence, a value of $(\Delta G^{\ddagger}_0)_{silver} = 10$ kcal/mol points to an inner-sphere contribution of ca. 5.5 kcal/mol, i.e., being about one-third of the difference $(\Delta G^{\ddagger}_0)_{inert} - (\Delta G^{\ddagger}_0)_{NC} = 15.5$ kcal/mol. This is consistent with the presence of an elongated carbon−chlorine bond in the primary intermediate though without undergoing a full rupture. Nevertheless, this intermediate is certainly highly unstable and presumably evolves within a few vibrations of its C−Cl bond which has certainly prevented its observation by SERS.

The fate of this first intermediate is described by the two limiting possibilities II-1 and II-2 which both lead to the same benzyl radical adduct characterized by SERS.[7] However, voltammetric data are now helpless in discriminating these two routes since they occur after the rate-determining step. Yet, by analogy with organometallic oxidative additions,[16] we favor this intermediate evolving through a concerted binding of the benzyl radical onto the silver surface (case II-2). Conversely, the alternative route II-1 would involve the formation of a free benzyl radical which then should bind competitively with its facile reduction[14] so as to afford the benzyl radical adduct observed by SERS. Though this cannot be disproved, it appears unlikely on the basis of the theoretical outcome of such competitions.[9] Indeed, in such a case, SERS should not yield any observable signal for the neutral benzyl adduct but should yield only that of the anionic benzyl adduct. Yet, the signal of the neutral species is clearly observed in SERS[7] showing that this species is a transient one involved in a dynamic steady state; this strongly suggests that the neutral benzyl adduct is formed directly on the silver surface upon fragmentation of the unstable bound anion radical. The fragmentation of this intermediate is expected to occur within a few vibrations of its weakened carbon−chlorine bond, while the exergonic reduction of the neutral benzyl adduct cannot proceed much more rapidly. It is then reasonable that such a situation may lead to a steady state dynamic concentration of the neutral benzyl adduct observable by SERS.

Within this framework, and irrespective of the issue of the competition between routes II-1 and II-2 (though we favor case II-2), the first reduction stage of benzyl chloride at silver electrodes may be viewed as a missing link, bridging the gap between activation of organic halides by electrochemical reduction at inert electrodes and by oxidative additions to homogeneous organometallic centers.[16]

Note that this mechanistic framework may be more general than the case investigated here though, to the best of our knowledge, this is the first time this is backed up by quantitative kinetic and spectroscopic evidence. Indeed, though generally forgotten in molecular electrochemistry, mechanistic sequences akin to those labeled II in Scheme 1 have been already proposed in an electrochemical context. This has for example been done in rationalizing the observation of smaller but drastically anodic prewaves during the reduction of several organic halides (RX) at a mercury electrode.[22] In such cases the main electrochemical wave observed at higher potentials proceeds through a sequence analogous to eqs 1−4, i.e., without involving chemically the mercury surface. Conversely, the drastically anodic prewaves were accounted for by the involvement of organomercury species resulting from oxidative addition (eq 26) taking place during the primary electron-transfer event:[22]

$$Hg^0_{cathode} + RX + e \rightarrow R\text{-}Hg^{I} + X^- \qquad (26)$$

$$R\text{-}Hg^{I} + RX + e \rightarrow R\text{-}Hg^{II}\text{-}R + X^- \qquad (27)$$

$$R\text{-}Hg^{II}\text{-}R \rightarrow R\text{-}R + "Hg^0" \qquad (28)$$

Within the present framework, the global eq 26 may indeed be viewed as a CE sequence involving a precomplexation-oxidative addition (C) leading to a transient organomercury intermediate continuously displaced by its facile reduction (E). The only difference with the process investigated in this work

(22) (a) Willett, B. C.; Peters, D. G. *J. Electroanal. Chem.* **1981**, *123*, 291–306. For related examples, see also the following reference. (b) Mbarak, M. S.; Peters, D. G. *J. Electroanal. Chem.* **1983**, *152*, 183–196. (c) Bart, J. C.; Peters, D. G. *J. Electroanal. Chem.* **1990**, *280*, 129–144.

(23) (a) Gennaro, A. *Electrocatalytic Reduction of Organic Halides, 60th Annual Meeting of the International Society of Electrochemistry*; Beijing, China; Keynote Lecture, August 18, 2009. (b) Note that there is a similar drastic positive shift of the reduction wave of aliphatic chloride at the silver electrodes when shifting from aprotic solvent to aqueous electrolytes; compare with the following: Scialdone, O.; Guarisco, C.; Galia, A.; Herbois, R. *J. Electroanal. Chem.* **2010**, *641*, 14–22.

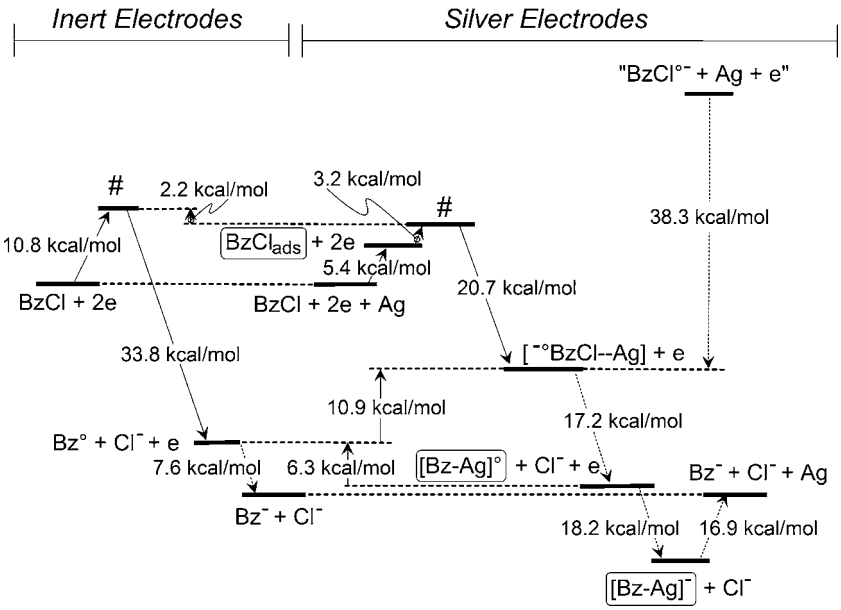

Figure 4. Scaled comparison between the energetics of the reaction pathways at inert and silver cathodes (note that the two initial systems have been arbitrarily set at the same energy to allow direct comparisons). The electron-transfer driving forces, Gibbs energies, and activation barriers have been evaluated at the voltammetric peak of benzyl chloride (BzCl) observed at silver electrodes at $\upsilon = 0.2$ V s^{-1} ($E^p = -1.76$ V versus SCE, Figure 1). Gibbs adsorption energies were taken from Table 1. Electron-transfer ones were evaluated as $(\Delta G)_{at\ Ep} = -F(E^p - E^\circ)$, where E° represents the standard potentials (vs SCE) of the redox couples of interest: $(E^\circ_1)_{inert} = -0.76$ V,[2a] $(E^\circ_2)_{inert} = -1.43$ V,[14] $(E^\circ_1)_{silver} = -1.0$ V, $(E^\circ_2)_{silver} = -0.97$ V, $(E^\circ_1)_{inert,NC} = -2.9$ V.[2a] Gibbs activation-barrier energies for the first reduction steps at each electrode were evaluated by using the expression $(\Delta G^\ddagger)_{at\ Ep} = \Delta G^\ddagger_0[1 + F(E^p - E^\circ)/(4\Delta G^\ddagger_0)]^2$, where $\Delta G^\ddagger_0$ is the corresponding intrinsic activation barrier: $(\Delta G^\ddagger_0)_{inert} = 20.7$ kcal/mol,[2a] $(\Delta G^\ddagger_0)_{silver} = 10.0$ kcal/mol. Direct dashed arrows are indicated for the second reduction steps since activation enthalpies are not known (see text). Intermediates directly observed by SERS[7a] are shown in solid frames.

is that the preceding step C in eq 26 is slow and limits kinetically the current intensity of the prewave.[13c] This intrinsic slowness suggests that, in agreement with the comparatively lower lattice energy of mercury versus silver, this C step is certainly a true oxidative addition (e.g., leading to a R−Hg^{II}−X species bound to the metal surface via its mercury center) rather than a weak adsorption as observed for benzyl chloride at silver electrodes. At silver cathodes, the C step has certainly a comparatively much weaker activation barrier and may then act as a fast uphill pre-equilibrium so that the prewave may fully develop and proceed under slow charge-transfer control.[12]

Similarly, Simonet et al. showed in a series of seminal works[11] that many electrode materials traditionally considered as inert, including noble metals, may lead to the formation of organic−metallic phases provided adequate electrochemical conditions are applied. These phases corrode the metal interface by forming reservoirs of organic radicals or anions which may be profitably used in electrochemical syntheses. Though not relevant to our studies, it is worth mentioning here that such results certainly establish that our classical vision of organic molecules at metal surfaces is still very limited.

Conclusion

Combining voltammetric, SERS, and DFT data has provided a coherent mechanistic framework (mechanisms II in Scheme 1, with mechanism II-2 being the most probable) to rationalize the exceptional catalytic properties of silver cathodes during the reduction of benzyl chloride. In this view, the large gain of ca. 0.5 V provided by silver electrodes results simultaneously from thermodynamic and kinetic factors. Both stem from specific interactions between the silver cathode surface and the substrate as well as with the primary product of the electron-transfer step. Interestingly, though this lowers the driving force of the electron-transfer step versus a concerted mechanism, this lowers drastically the intrinsic activation barrier of the rate-determining step.

As seen in Figure 4, the net result of these two contrasting effects is that at silver cathodes the overall CE sequence has a smaller effective activation barrier than the concerted pathway in eq 1. Hence this path is kinetically more efficient and enables the voltammetric wave to be displayed at drastically less negative potentials than at inert electrodes.

A quantitative analysis based on voltammetric data and previously reported ones relative to the concerted reduction of benzyl chloride at inert electrodes showed that, in contrast with the situation at inert electrodes, the first reduction proceeds through the formation of a fleeting species most certainly akin to an anion radical with an elongated carbon−halogen bond stabilized by the silver surface. In this view, this intermediate is located on the way between a free benzyl radical anion and the fully dissociated product pair, $PhCH_2^\bullet + Cl^-$, produced via the concerted electron transfer in eq 1. Such a species is thus expected to fragment within a few vibrations of its weakened carbon−chlorine bond presumably to afford the benzyl−silver radical adduct characterized by SERS[7a] (mechanism II-2). Thermodynamic and kinetic factors concur jointly in suggesting that this bound benzyl radical is easily reducible to a benzyl anion adduct also characterized by SERS.[7a] Hence, the voltammetric wave remains bielectronic over its entire potential span.[8c]

Finally, since the precomplexation of the substrate onto the silver surface is an uphill reaction, it has to be disfavored by the competitive adsorption of any other species (intermediate or products) prone to bind exergonically to the silver surface, as has been shown for the acetonitrile solvent and the 3-phenylpropanenitrile final product.[7a] This is also true for the benzyl

anion adduct intermediate which necessarily competes with the substrate precomplexation owing to its favorable adsorption. In this view, the potential location of the voltammetric wave may be regarded as resulting from a kinetic self-regulation between these two conflicting effects. If so, favoring any reaction prone to decrease the surface concentrations of the benzyl anion adduct and of the 3-phenylpropanenitrile product should favor the weaker adsorption of benzyl chloride, i.e., should provoke an even more positive shift of its reduction wave. It is worth mentioning in this respect a recent report from Gennaro et al.[23a] establishing that this is actually the case upon submitting the system to increasing concentrations of CO_2. This occurs most presumably due to a facile electrophilic attack envisioned in eq 29

$$[PhCH_2\text{-}Ag_n]^- + CO_2 \rightarrow PhCH_2\text{-}CO_2^- + Ag_n \qquad (29)$$

that occurs either on the surface (as in organometallic analog reactions[24]) or after desorption of the benzyl anion. Both paths would decrease the yield of 3-phenylpropanenitrile and favor the weak adsorption of benzyl chloride. In addition, if reaction 29 occurs directly on the surface, it would facilitate even more this weak binding by imposing a smaller steady-state surface concentration for the benzyl anion adduct. Water addition was also reported to lead to a large positive potential shift for the voltammetric reduction of alkyl halide reduction at silver cathodes,[23b] although the generated $PhCH_3$ has no affinity with the surface.[7] We thus favor the idea that electrophilic attacks of the anionic benzyl moiety by CO_2 (eq 29) or H_2O involve a direct reactivity between these electrophiles and the bound anionic adduct.

Besides the goal of unraveling the origin of the exceptional electrocatalytic effect of silver cathodes, this work also demonstrated that the integration of SERS measurements, DFT predictions, and voltammetric investigations offers a perfect triple tool for precise mechanistic investigations in molecular electrochemistry when unsuspected surface-bound intermediates are crucially involved.[12] SERS provides in situ molecular-level information to characterize nonclassical but key surface intermediates whose transient presence eludes voltammetric detection,[12] while the combination of voltammetry and DFT allows one to delineate how these species are kinetically involved in the mechanistic path.

Though intrinsically SERS-active metals are few, this does not limit the scope of this strategy. Indeed, various SERS-silent metals (such as iron, cobalt, nickel, platinum, and palladium)[25] may be turned into SERS-active materials through the use of core−shell nanoparticles in which the SERS-silent metal of interest is "wrapped" around a core of a SERS-active one.[26] Such core−shell nanoparticles have been shown to provide sufficiently large enhancement factors ($\sim 10^4$ to 10^5)[26] that allow investigations with an accuracy similar to the present one. Furthermore, very recently, a new technique (shell-isolated nanoparticle-enhanced Raman spectroscopy, SHINERS) has been developed to investigate electrochemical adsorption and reaction on single-crystal surfaces of various metal electrodes.[27] This opens new frontiers in many areas of electrochemical interest as well as many others in which catalytic interactions between reactants and metal surfaces are determinant, and provides additional means to explore even further the gap between classical electrochemical activation and organometallic catalysis.

Experimental Section

Materials and Reagents. Commercial acetonitrile solvent (AR grade, SCRC Co. Ltd.) was used without further purification. TEAP (electrochemical grade, Alfa Aesar) and benzyl chloride (AR grade, SCRC Co. Ltd.) were also used without further purification.

Voltammetric Measurements. All electrochemical experiments were carried out with silver wires (2 mm diameter; 99.999% from Alfa Aesar), which were sealed into a Teflon (polytetrafluoroethylene) stick. The silver electrode was polished to a mirror finish with emery paper of decreasing grain size followed by alumina powder with 3, 1, and 0.3 μm particle sizes in this sequence. A three-electrode electrochemical cell was used in which the reference electrode was a home-built Ag/Ag^+ pseudoreference electrode and the counter electrode was a Pt wire. For convenience and comparison to previous results published in the literature, all potentials have been converted to the SCE scale by subtracting a 45 mV potential difference as determined by independent calibration performed after the measurements.

Voltammetric signals were imposed to the cell by a potentiostat (CHI 631B,CH Instrument); currents and potential data were stored on a computer hard disk for further processing.

DFT Calculations. Cluster models including silver clusters with different sizes of Ag_n ($n = 1-5$ and 10) were used in the DFT computations as models of the silver electrode surface for optimizing the structures of surface complexes of possible intermediates and products. DFT calculations were performed with the hybrid exchange functional of Becke's 3 parameters (B3) and Lee−Yang−Parr's nonlocal correlation functional (LYP) for finding the stable optimization geometries and calculating vibrational spectra.[28,29] Basis sets for C, Cl, and H were 6-311+G** with polarization functions for C, Cl, and H, and with diffuse function only for C and Cl atoms. For silver atoms, the valence and core electrons were described by the basis set of LanL2DZ and the corresponding relativistic effective core potential (ECP), respectively.[28] The solvent effect was considered by the integral equation formal polarization continuum model (IEF-PCM).[15] All calculations concerning the geometry optimization were performed with the aid of the Gaussian09 software package.[15] The ensuing geometries are described in the Supporting Information material of ref 7a.

Thermodynamic adsorption energies of the benzyl chloride, benzyl radical, benzyl anion, and acetonitrile have been evaluated on silver atom clusters (Ag_n, $n = 1-5$ and 10) without considering the role of the solvent. This showed that $n = 4$ was sufficient to provide correct bonding contributions compared to more extended clusters. Furthermore, we selected Ag_4 clusters to simulate the electrode owing to its structural stability when it was negatively charged. Indeed, even nowadays it is still very difficult to evaluate thermodynamic energies of an electrochemical system by DFT, mostly because of the difficulty of accounting for the electrode potential. The strategy we used is that commonly adopted by the whole community. It relies on defining suitable atomic clusters and adding charges to them in order to represent the electrode charge density. In a series of preliminary tests we observed that upon adsorption of the organic moieties such negative charging led to

(24) (a) Amatore, C.; Jutand, A. *J. Am. Chem. Soc.* **1991**, *113*, 2819–2825. (b) Amatore, C.; Jutand, A.; Khalil, F.; Nielsen, M. F. *J. Am. Chem. Soc.* **1992**, *114*, 7076–7085.
(25) (a) Tian, Z. Q.; Ren, B. *Annu. Rev. Phys. Chem.* **2004**, *55*, 197–229. (b) Tian, Z. Q.; Ren, B.; Wu, D. Y. *J. Phys. Chem. B* **2002**, *106*, 9463–9483.
(26) Wu, D. Y.; Li, J. F.; Ren, B.; Tian, Z. Q. *Chem. Soc. Rev.* **2008**, *37*, 1025–1041.
(27) Li, J. F.; Huang, Y. F.; Ding, Y.; Yang, Z. L.; Li, S. B.; Zhou, X. S.; Fan, F. R.; Zhang, W.; Zhou, Z. Y.; Wu, D. Y.; Ren, B.; Wang, Z. L.; Tian, Z. Q. *Nature* **2010**, *464*, 392–395.
(28) Lee, C.; Yang, W.; Parr, R. G. *Phys. Rev. B* **1988**, *37*, 785–789.
(29) Hay, P. J.; Wadt, W. R. *J. Chem. Phys.* **1985**, *82*, 299–310.

geometric deformations in some Ag clusters. Although this did not alter significantly the structures of organic moieties in the adducts, this created a problem in estimating the adsorption thermodynamics. However, this problem was found to be minimal for the Ag_4 cluster used in the present paper. Furthermore, other functionals (B3PW91 or X3LYP)[30] have been used to estimate these values and provided similar results ($\pm$0.5 kcal/mol for the $PhCH_2Cl-Ag_4$ adduct) to those reported in Table 1.

Hence, Ag_4 clusters were used to simulate the active adsorption site on the electrode and more extensive calculations including a solvent continuum model were performed (see Supporting Information in ref 7a). Adsorption energies and entropies reported in Table 1 were then obtained from the equation

$$\Delta SF_{adsorb} = SF_{X-Ag_4} - SF_X - SF_{Ag_4}$$

where "SF" represents the standard thermodynamic function of interest.

Acknowledgment. This work is dedicated to the memory of the late Jay K. Kochi. It was supported in part by CNRS, UPMC, and ENS (UMR 8640 and LIA XiamENS) in France and by NSFC (20620130427) and MOST (2007DFC40440) in China.

Supporting Information Available: Complete ref 15 including all authors. This material is available free of charge via the Internet at http://pubs.acs.org.

JA106049C

(30) (a) Perdew, J. P.; Burke, K.; Wang, Y. *Phys. Rev. B* **1996**, *54*, 16533. (b) Xu, X.; Goddard, W. A. *Proc. Natl. Acad. Sci. U.S.A.* **2004**, *101*, 2673–2677.